virtue of their known activity against plasminogen activators, their role as tumor suppressors in breast cancer is not established (*20*). Similarly, the activity of metalloproteinase inhibitors in breast cancer is not yet known (*21*).

From a clinical perspective, maspin offers substantial opportunities. First, the loss of expression that occurs during malignant progression of primary tumors suggests that maspin has potential value as a marker of a favorable prognosis. Maspin may also have therapeutic potential. The maspin gene is not lost in tumor cells but rather is down-regulated, as shown by the partial loss of expression in primary carcinomas and by its up-regulation in tumor cells after treatment with a phorbol ester (*9*). Maspin offers the potential of novel pharmacological approaches to therapy, such as inducing re-expression of the protein in breast cancers or blocking expression of the target protease.

REFERENCES AND NOTES

1. R. Sager, *Science* **246**, 1406 (1989).
2. S. W. Lee, C. Tomasetto, R. Sager, *Proc. Natl. Acad. Sci. U.S.A.* **88**, 2825 (1991).
3. S. W. Lee, C. Tomasetto, K. Swisshelm, K. Keyomarsi, R. Sager, *ibid.* **89**, 2504 (1992).
4. S. Lee, C. Tomasetto, D. Paul, K. Keyomarsi, R. Sager, *J. Cell Biol.* **118**, 1213 (1992).
5. C. Tomasetto, M. S. Neveu, J. Daley, P. K. Horan, R. Sager, *ibid.* **122**, 157 (1993).
6. P. Liang, L. Averboukh, K. Keyomarsi, R. Sager, A. B. Pardee, *Cancer Res.* **52**, 6966 (1992).
7. R. Sager, A. Anisowicz, M. Neveu, P. Liang, G. Sotiropoulou, *FASEB J.* **7**, 964 (1993).
8. V. Band and R. Sager, *Proc. Natl. Acad. Sci. U.S.A.* **86**, 1249 (1989).
9. Z. Zou *et al.*, unpublished observations.
10. M. Kozak, *Nucleic Acids Res.* **12**, 857 (1984).
11. J. Travis, A. Guzdek, J. Potempa, W. Watorek, *Biol. Chem. Hoppe Seyler* **371**, 3 (1990).
12. R. Huber and R. W. Carrell, *Biochemistry* **28**, 8951 (1989).
13. E. Harlow and D. Lane, in *Antibodies: A Laboratory Manual* (Cold Spring Harbor Laboratory, Cold Spring Harbor, NY, 1988), chap. 8.
14. J. E. Price, A. Polyzos, R. D. Zhang, L. M. Daniels, *Cancer Res.* **50**, 717 (1990).
15. At 10 weeks after inoculation, all mice were killed and their tumors excised and weighed. Lymph nodes adjacent to the site of injection and lungs were also removed and preserved for histological examination. Multiple 5-μm sections of lung and lymph nodes from each animal were stained with hematoxylin and eosin. Specimens were coded, and their identity was unknown to the pathologist.
16. M. J. C. Hendrix, E. A. Seftor, R. E. B. Seftor, I. J. Fidler, *Cancer Lett.* **38**, 137 (1987).
17. S. Sheng and R. Sager, unpublished observations.
18. L. Liotta and W. G. Stetler-Stevenson, *Cancer Res.* **51**, 5054 (1991).
19. M. J. C. Hendrix, unpublished observations.
20. J. E. Testa and J. P. Quigley, *Cancer Metastasis Rev.* **9**, 353 (1990).
21. W. G. Stetler-Stevenson, S. Aznavoorian, L. A. Liotta, *Annu. Rev. Cell Biol.* **9**, 541 (1993).
22. Abbreviations for the amino acid residues are A, Ala; C, Cys; D, Asp; E, Glu; F, Phe; G, Gly; H, His; I, Ile; K, Lys; L, Leu; M, Met; N, Asn; P, Pro; Q, Gln; R, Arg; S, Ser; T, Thr; V, Val; W, Trp; and Y, Tyr.
23. The ability of maspin-transfected clones (T1 to T7) to penetrate Matrigel-coated (Becton Dickinson, Boston, MA) polycarbonate filters (containing 10-μm pores) was measured with the membrane invasion culture system (MICS) (*16*). Cells (1×10^5) were seeded into the upper wells of the MICS chamber onto the Matrigel-coated filter in Dulbecco's minimum essential medium containing 10% NuSerum (Becton Dickinson). After 72 hours of incubation at 37°C with constant O_2 and CO_2 exchange, the cells that invaded the filter were collected, stained, and counted.
24. J. C. Adams, *J. Histochem. Cytochem.* **40**, 1457 (1992).
25. We thank P. Pemberton for advice on serpin structure; H. B. Warren for histopathologic examination of animal tissues; A. B. Pardee, B. Zetter, and C. Li for helpful suggestions; K. Ryan for technical assistance; and M. Connolly for preparing the manuscript. Supported by NIH grants to R.S. (PO1 CA22427 and OIG CA39814) and to M.J.C.H. (RO1 CA59702). M.N. was a recipient of an Interdisciplinary Program in Health Fellowship from the Harvard School of Public Health.

2 November 1993; accepted 15 December 1993

Visualization of Quantal Synaptic Transmission by Dendritic Calcium Imaging

Timothy H. Murphy,* Jay M. Baraban, W. Gil Wier, Lothar A. Blatter†

As changes in synaptic strength are thought to be critical for learning and memory, it would be useful to monitor the activity of individual identified synapses on mammalian central neurons. Calcium imaging of cortical neurons grown in primary culture was used to visualize the activation of individual postsynaptic elements by miniature excitatory synaptic currents elicited by spontaneous quantal release. This approach revealed that the probability of spontaneous activity differed among synapses on the same dendrite. Furthermore, synapses that undergo changes in activity induced by glutamate or phorbol ester treatment were identified.

Miniature excitatory synaptic currents (MESCs) are a fundamental form of neuronal communication produced by the spontaneous release of a single transmitter quantum (*1*). Experiments suggest that at central synapses a single MESC is equivalent to a postsynaptic response resulting from the evoked activation of a single synaptic terminal (*2*). By analogy with quantal analysis used to define mechanisms of synaptic plasticity at neuromuscular junctions, analysis of MESCs has been used to provide information about changes in release probability and postsynaptic responsiveness in models of plasticity in brain neurons (*1*). Prompted by concerns that assumptions implicit in these analyses may not be applicable to populations of central synapses (*3*), we have visualized postsynaptic calcium transients induced by MESCs to monitor activity at individual synapses.

For this approach we used rat cerebral cortical neurons grown in primary culture (*4*, *5*) because they form functional synapses and exhibit synaptically induced free cytoplasmic Ca^{2+} $[Ca^{2+}]_i$ transients in postsynaptic dendritic processes detectable in neurons microinjected with the Ca^{2+}-sensitive probe fura 2 (*6*–*8*). In the presence of tetrodotoxin (TTX) and the absence of extracellular Mg^{2+} (*4*), highly localized $[Ca^{2+}]_i$ transients, which we termed miniature synaptic calcium transients (MSCTs), were observed in spiny distal dendritic segments (Fig. 1). The MSCTs arose from an initial focal point of 1 to 2 μm^2 and spread along the dendritic axis to produce a $[Ca^{2+}]_i$ elevation that extended ~10 μm. The distance between synaptic terminals aligned on a dendrite and labeled with synaptophysin or rhodamine 123 was estimated to be 2.3 ± 0.7 and 2.7 ± 0.9 μm (mean ± SD), respectively (*9*). Thus, the highly localized initiation of the MSCTs likely reflects spontaneous quantal release from a single presynaptic terminal and the subsequent $[Ca^{2+}]_i$ transient in the postsynaptic dendrite.

MSCTs appeared to be mediated by activation of *N*-methyl-D-aspartate (NMDA) receptors by released glutamate (Glu), because in the presence of the competitive antagonist DL-2-amino-5-phosphonovaleric acid (DL-APV) (*10*), no MSCTs occurred in 21 10-s trials. In contrast, in untreated cultures 60 MSCTs were observed in 71 10-s trials. The effects of DL-APV were reversible: synaptically mediated $[Ca^{2+}]_i$ transients were observed after DL-APV was removed.

To ensure that the spatially restricted nature of the MSCTs was not due to the inability of some postsynaptic elements to exhibit elevations in $[Ca^{2+}]_i$, we also imaged these dendrites in the absence of TTX to monitor synaptic $[Ca^{2+}]_i$ transients (SCTs) produced by synchronous action

T. H. Murphy and J. M. Baraban, Department of Neuroscience, Johns Hopkins University School of Medicine, Baltimore, MD 21205.
W. G. Wier and L. A. Blatter, Department of Physiology, University of Maryland School of Medicine, Baltimore, MD 21201.

*To whom correspondence should be addressed.
†Present address: Department of Physiology, Loyola University Chicago, Maywood, IL 60153.

potential–dependent synaptic activity. The detection of relatively homogeneous $[Ca^{2+}]_i$ transients over the entire dendritic segment during SCTs (Fig. 2A) (6) suggests that all postsynaptic sites are responsive.

To better understand the relation between MSCTs and SCTs, we compared their kinetics (Fig. 2B) and sensitivity to NMDA receptor blockade (6) and found that they are similar. These similarities suggested that, to a first approximation, the spatial summation of multiple MSCTs could underlie evoked synaptic responses in fine dendritic processes. For example, two MSCTs occurring in close temporal succession produced a relatively homogeneous rise in $[Ca^{2+}]_i$ in the intervening segment (Fig. 1A).

Whole cell recordings made with the same solutions used in the imaging studies indicated the presence of MESCs (6 to 50 pA) (*11, 12*) that were dependent on Glu receptors, as local or bath application of the broad spectrum ionotropic Glu receptor antagonist kynurenate greatly reduced their amplitude (*13*). The mean frequency of these currents (2.1 ± 0.5 Hz) was within the range of estimated frequencies for MSCTs per neuron (1 to 5 Hz) (*14*).

In the course of these imaging studies, multiple MSCT events often occurred at the same dendritic site (Fig. 1). Statistical analysis of these repeated MSCTs indicated that they are not explained by random behavior (*15*). At a high probability site (denoted B in Fig. 1A), five of nine total MSCTs were observed (the probability of this occurring at any one site randomly is 0.003). A total of 26 different dendritic fields were examined in which 49 distinct MSCT sites were observed. Of these sites, 14 displayed more than one MSCT. For each of these 14 sites, we calculated the probability of the repeated events occurring randomly at that specific site (*15*). In 11 of the 14 cases, the probability of repeated events at these identified specific sites was less than 0.05, suggesting that these sites have a higher probability of spontaneous activity than others within the population. However, from our data it is not possible to determine whether the heterogeneous distribution of MSCTs is due to differences in the rate of spontaneous transmitter release (*1, 16, 17*) or in postsynaptic responsiveness (*18*).

The presence of synapses with a high probability of spontaneous activity could indicate that they had undergone activity-dependent plasticity. Because the cultures used in the experiments illustrated in Fig. 1 were routinely synaptically stimulated (picrotoxin-induced bursting) (*5, 6*) for at least 15 min, 0.5 hour, and 3 hours before

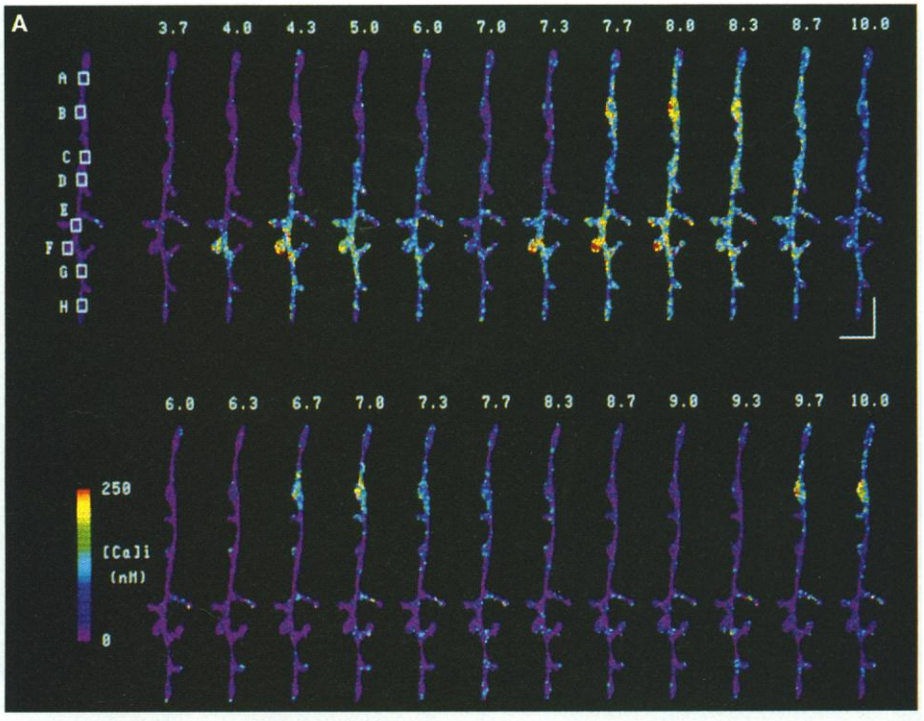

Fig. 1. The $[Ca^{2+}]_i$ transients associated with quantal release. (**A**) Images shown in each row reflect $[Ca^{2+}]_i$ at the indicated times in a 10-s run. As shown in the top row, this dendrite exhibited three separate local increases in $[Ca^{2+}]_i$ within the 10-s sampling period. The first transient is initiated at a spine (site F) at t = 4 s. Over the next 1 s, the rise in $[Ca^{2+}]_i$ spreads to involve ~10 μm of the dendrite and four to five other spines. Another MSCT is observed at site F at t = 7.3 s. At t = 7.7 s, an independent $[Ca^{2+}]_i$ transient originated at site B. Over the next few seconds, the rise in $[Ca^{2+}]_i$ overlaps in the segment connecting them. In the next 10-s sample shown in the bottom row (done ~10 min later), $[Ca^{2+}]_i$ returned to basal concentrations before the appearance of two additional MSCTs at site B. The plane of focus was adjusted slightly for the second run, accounting for the structural differences between the two panels. Calibration = 5 μm; the small boxes are 1.8 μm^2 or 63 pixels. (**B**) Plots of $[Ca^{2+}]_i$ as a function of time are displayed for the run shown in the top row for eight sites indicated in the first image in (A). The dashed lines mark the beginning of MSCT events.

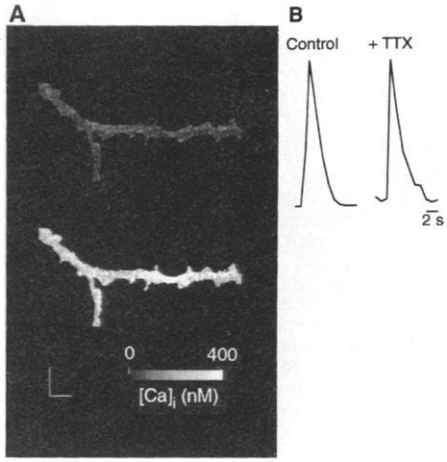

Fig. 2. Synchronous and local synaptic activation of dendrites. (**A**) A single cortical neuron was injected with fura 2 as described in Fig. 1, and ratiometric imaging was done in a fine spiny dendritic process before (top) and during a burst of action potential–dependent spontaneous synchronous synaptic activity. In the absence of TTX, $[Ca^{2+}]_i$ rose relatively homogeneously in fine dendrites of all neurons examined (n = 5). Calibration = 5 μm. (**B**) Comparison of MSCTs with synaptic $[Ca^{2+}]_i$ transients (SCTs). The $[Ca^{2+}]_i$ imaging was done in a fine spiny dendritic process during action potential–dependent synaptic activity (SCT) and during miniature synaptic activity (MSCT). Three $[Ca^{2+}]_i$ transients were recorded under each condition, averaged, and normalized to a peak of 100%. Comparison of their time courses indicated that SCTs (control) and MSCTs (TTX) have similar kinetics.

recording MSCTs, we examined whether unstimulated cultures would have a lower number of these apparent high probability synapses and whether stimulation of these cultures could change the incidence of MSCTs. For these experiments, we kept cultures in a quiescent state with TTX for at least 3 hours before assessing MSCTs. Under these conditions, we recorded from eight neurons and detected 17 sites with repeated MSCTs. At only two of these sites we found $P < 0.05$ (as defined above for the 14 cases). This suggested that previous bursting activity induced an increase in the probability of spontaneous activity in a subset of synapses.

In addition, under these quiescent conditions treatment with Glu or a phorbol ester, agents which have been shown to augment evoked synaptic activity (*17, 19*) and MESCs (*11, 17*), could alter the distribution of spontaneous MSCTs. Treatment with Glu, which consisted of two 20-s pulses of locally applied Glu (20 to 50 μM), produced an increase in the number of high probability sites (none in control and four after Glu, $n = 4$ neurons) (*15*) with no significant effect on MSCT frequency (111 ± 4% of control, $n = 4$ neurons, mean ± SEM) or the number of active sites (96 ± 27% of control, $n = 4$ cells). Under control conditions six MSCTs occurred at six different locations (Fig. 3); 5 to 10 min after Glu treatment, seven of eight total MSCTs occurred at a single dendritic spine (the probability of this occurring randomly at any one of the six active sites is 0.0003), suggesting an increase in synaptic strength at that specific location. Phorbol ester treatment [continuous bath application of 2 μM phorbol 12,13-diacetate (PDA)] produced a statistically significant increase ($P < 0.05$, one-factor analysis of variance) in MSCT frequency (201 ± 34% of control, $n = 4$ cells) and the number of MSCT sites (160 ± 25% of control, $n = 4$). Treatment with PDA also increased the number of specific sites with a binomial probability (*15*) less than 0.05 (one site in control 3 after PDA treatment).

Our results suggest a model in which each synapse has a characteristic rate of quantal synaptic transmission. At some synapses this rate appears to be subject to experience-dependent modification (Fig. 3). To address this hypothesis, we examined the distribution of MSCT rates at single identified synapses (*20*). In unstimulated cultures, the distribution of MSCT rates ranged from zero to three events per site and agreed well with that expected for random occurrence at relatively equivalent sites. However, with synaptic stimulation, phorbol ester treatment, or Glu application, the distribution became broader and included sites with rates ranging from zero to six events per site. In these stimulated cultures the distribution was no longer consistent with random Poisson behavior.

Our studies, consistent with previous reports (*21, 22*), indicate that NMDA receptors mediate dendritic synaptic $[Ca^{2+}]_i$ transients. However, in contrast to some studies (*22, 23*), we often observed that dendritic spines did not confine Ca^{2+} movement. Conceivably, this difference may be due to development in vitro of neurons used for this study. In our studies, the extent of MSCT propagation frequently encompassed several synapses, suggesting that activity at one synapse can influence another. It is possible that synapse specificity, a common tenet of plasticity models, might not be strictly controlled at the dendritic spine level (*24*) but at small domains of synapses defined by the spread of $[Ca^{2+}]_i$. Because pyramidal neurons can have greater than 10,000 μm of linear dendrite (*25*), hundreds of these units could exist.

Recent electrophysiological studies indicate that release probability can vary widely among central synapses innervating a single neuron (*26*). The ability to visualize individual synapses with different probabilities of activity by MSCT imaging may allow future studies to be directed toward elucidating the structural and biochemical alterations that underlie these differences.

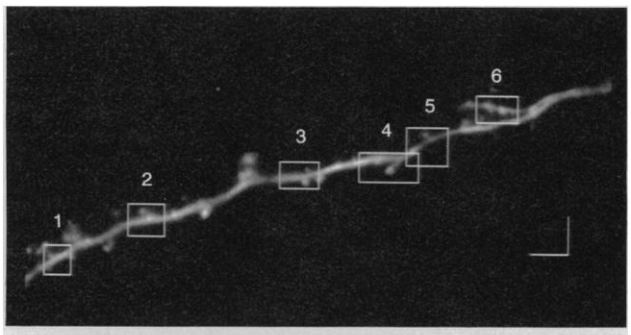

Frequency (Hz)	Location					
	1	2	3	4	5	6
Control	0.025	0.025	0.025	0.025	0.025	0.025
Glutamate	0	0	0	0.14	0	0.02

Fig. 3. Location of a high probability synapse induced by Glu treatment. A 360-nm fura 2 image of a cortical neuron dendrite is shown. The neuron was kept under quiescent conditions for ~3 hours before MSCTs were recorded. Four control runs of 10-s duration were made in which six MSCTs were observed at six different sites. The approximate boundaries of their $[Ca^{2+}]_i$ transients are shown by boxes. Approximately 2 min after the last control run, the dendrite was exposed to two 20-s pulses of Glu (20 μM; separated by ~1 min, applied by pressure ejection with a locally placed pipette). The effect of Glu was confirmed by observation of a large $[Ca^{2+}]_i$ transient that encompassed the whole dendrite. Four minutes after $[Ca^{2+}]_i$ had returned to control concentrations, MSCTs were assessed at 90-s intervals (five 10-s runs were recorded). After Glu treatment seven of eight total MSCTs observed occurred at the same site (initiated at the spine in location 4). The probability of seven of eight events occurring at any one of six locations randomly (a conservative assumption, as greater than six sites are indicated by spines) was calculated to be 0.0003. In the absence of Glu stimulation, the frequency of MSCT events and the number of high probability sites within a dendritic field were stable over time. For example, in a neuron not treated with Glu, 14 MSCT events were observed with no apparent high probability sites (*15*) in eight runs; 30 min later, 15 MSCT events were observed without the appearance of high probability sites in the same number of sampling runs. Calibration = 5 μm.

REFERENCES AND NOTES

1. C. F. Stevens, *Cell* **72** (suppl.), 55 (1993); J. E. Lisman and K. M. Harris, *Trends Neurosci.* **16**, 141 (1993).
2. N. Otmakhov, A. M. Shirke, R. Malinow, *Neuron* **10**, 1101 (1993); M. Raastad, J. F. Storm, P. Andersen, *Eur. J. Neurosci.* **4**, 113 (1992).
3. F. A. Edwards, A. Konnerth, B. Sakmann, *J. Physiol.* **430**, 213 (1990); D. S. Faber, W. S. Young, P. Legendre, H. Korn, *Science* **258**, 1494 (1992); A. Larkman, K. Stratford, J. Jack, *Nature* **350**, 344 (1991).
4. Cortical neurons and glia were dissociated from 17- to 18-day gestation rat fetuses, placed in culture, and allowed to mature for at least 17 to 26 days in vitro as described (*5*). Cortical neurons were impaled with 40- to 60-Mohm microelectrodes that were filled (tip only) with 10 mM fura 2 (K^+ salt, Molecular Probes) in 200 mM KCl (*6*). Electrodes were then removed and the cells allowed to recover in the presence of TTX for about 2 to 3 hours before assessment of $[Ca^{2+}]_i$. Ratiometric fura 2 imaging was then done at room temperature (*6–8*). Images are the average of four consecutive video frames. These averaged images were acquired every 333 ms. Thus, in a typical 10-s run, 30 images were collected. The following extracellular solution was used to isolate MESCs: 137 mM NaCl, 5.0 mM KCl, 5.0 mM $CaCl_2$, 0.44 mM KH_2PO_4, 0.34 mM $Na_2HPO_4(7H_2O)$, 10 mM Na^+ Hepes, 1 mM $NaHCO_3$, picrotoxin (0.01 mM), tetrodotoxin (0.001 mM), and 22 mM glucose (pH 7.4 and 340 mosM). To facilitate the observation of MSCTs, we removed extracellular Mg^{2+}, which mimics effects of depolarization on NMDA receptor function. Thus, under physiological conditions, if a neuron were depolarized by activity at distant synapses, coincident activity at a single synapse could then elicit local NMDA receptor–mediated Ca^{2+} influx that would be expected to have characteristics similar to the transients we observed in the absence of Mg^{2+}.

Extracellular $CaCl_2$ was elevated to 5 mM to increase Ca^{2+} influx through the NMDA receptor. The concentration of KCl and osmolarity used were based on the minimal essential medium these neurons were cultured in. Cells were switched to this solution from Hanks balanced salt solution at least 10 min before MSCT imaging.
5. T. H. Murphy, L. A. Blatter, W. G. Wier, J. M. Baraban, *J. Neurosci.* **12**, 4834 (1992).
6. T. H. Murphy *et al.*, *ibid.* **14**, 1320 (1994).
7. L. A. Blatter and W. G. Wier, *Am. J. Physiol.* **263**, 576 (1992).
8. G. Grynkiewicz, M. Poenie, R. Y. Tsien, *J. Biol. Chem.* **260**, 3440 (1985).
9. B. Wiedermann and W. W. Franke, *Cell* **41**, 1017 (1985); D. Yoshikami and L. M. Okun, *Nature* **310**, 53 (1984). Values presented are the mean ± SD obtained from counting labeled terminals on 27 dendritic segments of five neurons for rhodamine 123 and 26 segments of four neurons for synaptophysin.
10. We used 200 μM of the racemic DL-APV. This provided a saturating concentration of the active (D) isomer to ensure complete blockade of the NMDA receptor responses. In previous studies with this preparation, we observed that this concentration did not abolish rhythmic calcium transients produced in neuronal cell bodies that are dependent on the activation of non-NMDA glutamate receptors (*13*).
11. D. M. Finch and M. B. Jackson, *Brain Res.* **518**, 269 (1990).
12. J. M. Bekkers and C. F. Stevens, *Nature* **341**, 230 (1989).
13. T. H. Murphy, J. M. Baraban, W. G. Wier, L. A. Blatter, unpublished results.
14. We calculated the frequency of MSCTs per neuron assuming an average dendritic length imaged of 200 μm per neuron and a total dendritic length of 3000 μm per neuron (estimated from three biocytin-filled neurons). MSCT frequency estimates were based on data from eight neurons used as controls in the glutamate and phorbol ester studies.
15. The probability of repeated events at a specific dendritic site was calculated with the binomial equation $P = n!/y!(n - y)![p^y(1 - p)^{n-y}]$, where y is the number of MSCTs observed at a particular site and p is the probability of an event occurring at a particular site within a single trial, assuming independent random behavior. We considered the release and action of a transmitter quantum to be equivalent to a trial (n); that is, if nine MSCTs were observed, $n = 9$. To calculate the value of p, we estimated the number of synaptic sites in a typical dendritic segment that was used for imaging studies. In these experiments, dendritic segments that averaged 205 ± 22 μm in length were imaged (images in all figures are not full frames), which contained ~80 synapses (see text). If the location at which MSCTs occurred was random, the probability of an event at any single site would be 1/80. Because it was difficult to always discriminate events occurring at adjacent synapses, we used the conservative assumption that at least thirteen 15-μm segments could be resolved in each dendrite sampled. Therefore, the probability of an event in a 15-μm segment was 0.075 (15/200).
16. J. M. Bekkers and C. F. Stevens, *Nature* **346**, 724 (1990); T. V. P. Bliss and G. L. Collingridge, *ibid.* **361**, 31 (1993); R. Robitaille and J. P. Tremblay, *Neuroscience* **40**, 571 (1991).
17. A. Malgaroli and R. W. Tsien, *Nature* **357**, 134 (1992).
18. T. Manabe, P. Renner, R. A. Nicoll, *ibid.* **355**, 50 (1992).
19. R. J. Cormier, M. D. Mauk, P. T. Kelly, *Neuron* **10**, 907 (1993); R. C. Malenka, D. V. Madison, R. A. Nicoll, *Nature* **321**, 175 (1986).
20. In experiments that exhibited more than three MSCT events, we determined the number of events at each site that showed activity for the four 10-s sampling epochs typically used. Values from different experiments were pooled, and a distribution histogram of sites with 0, 1, 2, 3, 4, 5, and 6 MSCT events was created. Data were obtained from eight separate control experiments from quiescent unstimulated cultures (n = 68 events); nine separate experiments from synaptically stimulated cultures (n = 69 events); and four separate experiments from Glu- or phorbol ester–treated cultures (n = 49 and 47 events, respectively). Expected values were calculated with the Poisson equation $P = ne^{-m}m^K/K!$, where n is the total number of presumed sites (assumed to be 13 for each experiment), m is the mean number of events per site, and K is the number of events 0 to 6. The observed values were not significantly different from the expected distribution for unstimulated cultures, as indicated by χ^2 analysis ($\alpha > 0.1$); however, expected values (for synaptically stimulated cultures and cultures stimulated with Glu or phorbol ester) were significantly different from those observed ($\alpha < 0.025$).
21. W. G. Regehr and D. W. Tank, *Nature* **345**, 807 (1990).
22. W. Muller and J. A. Connor, *ibid.* **354**, 73 (1991).
23. P. B. Guthrie, M. Segal, S. B. Kater, *ibid.*, p. 76.
24. C. Koch and A. Zador, *J. Neurosci.* **13**, 413 (1993).
25. D. G. Amaral, N. Ishizuka, B. Claiborne, *Prog. Brain Res.* **83**, 1 (1990).
26. C. Rosenmund, J. D. Clements, G. L. Westbrook, *Science* **262**, 754 (1993); N. A. Hessler, A. M. Shirke, R. Malinow, *Nature* **366**, 6455 (1993).
27. Supported by grants from the USPHS and the American Heart Association, Maryland affiliate. We thank D. Rodgers for secretarial assistance and D. Linden, D. Yue, D. Blake, and L. Raymond for helpful comments.

4 October 1993; accepted 7 December 1993

Locally Distributed Synaptic Potentiation in the Hippocampus

Erin M. Schuman*† and Daniel V. Madison

The long-lasting increase in synaptic strength known as long-term potentiation has been advanced as a potential physiological mechanism for many forms of both developmental and adult neuronal plasticity. In many models of plasticity, intercellular communication has been proposed to account for observations in which simultaneously active neurons are strengthened together. The data presented here indicate that long-term potentiation can be communicated between synapses on neighboring neurons by means of a diffusible messenger. This distributed potentiation provides a mechanism for the cooperative strengthening of proximal synapses and may underlie a variety of plastic processes in the nervous system.

Most models of neuronal development, learning, memory, and circuit reorganization include alterations of the strength of synaptic connections between neurons. These models suggest that communication occurs between like synapses, such that synapses that are coactive tend to function as a group (*1*). Long-term potentiation (LTP), the long-lasting increase in synaptic transmission that is induced by intense synaptic activity (*2*), has been advanced as a potential physiological mechanism for these forms of plasticity. Although LTP clearly results in enhanced synaptic transmission, it is less clear whether it possesses the properties necessary to mediate the intercellular communication inherent in most models of coactive strengthening. When LTP is selectively induced in one synaptic pathway, other synaptic inputs to the same cell do not undergo LTP (*3*). This input specificity has usually been interpreted to mean that potentiation cannot be communicated from one synapse to another.

During the induction of LTP, postsynaptic events such as *N*-methyl-D-aspartate (NMDA) receptor activation and Ca^{2+} influx have been suggested to lead to the generation of different diffusible signals (*4*), such as arachidonic acid (*5*), carbon monoxide (*6*), nitric oxide (NO) (*7–9*), and platelet-activating factor (*10, 11*). These signals have been proposed to mediate the synaptic enhancement of LTP (*5–13*). In theory, a diffusible messenger could act in a strictly retrograde manner, influencing only the synapses where it is generated, or it could diffuse to enhance the synapses of nearby neurons as well. Indeed, an LTP induction procedure, pairing postsynaptic depolarization of a single neuron with low-frequency stimulation of afferent fibers (*14*) decreases the action potential latency in both the depolarized cell as well as nearby cells (*15, 16*).

To examine whether long-lasting synaptic potentiation could spread to nearby synapses in hippocampal slices, we made simultaneous intracellular recordings from two nearby CA1 pyramidal neurons and monitored the excitatory postsynaptic potentials (EPSPs) resulting from stimulation of Schaffer collaterals (*17*) (Fig. 1A). We detected no synaptic or electrical coupling

Department of Molecular and Cellular Physiology, Beckman Center for Molecular and Genetic Medicine, Stanford Medical School, Stanford, CA 94305.

*Present address: Division of Biology 216-76, California Institute of Technology, Pasadena, CA 91125.
†To whom correspondence should be addressed.